Journal of Hazardous Materials 164 (2009) 271–278

Contents lists available at ScienceDirect

Journal of Hazardous Materials

journal homepage: www.elsevier.com/locate/jhazmat

Removal of fluoride from water by using granular red mud: Batch and column studies

Ali Tor[a,*], Nadide Danaoglu[a], Gulsin Arslan[b], Yunus Cengeloglu[b]

[a] Selcuk University, Department of Environmental Engineering, Campus, 42031 Konya, Turkey
[b] Selcuk University, Department of Chemistry, Campus, 42031 Konya, Turkey

ARTICLE INFO

Article history:
Received 13 May 2008
Received in revised form 1 August 2008
Accepted 1 August 2008
Available online 14 August 2008

Keywords:
Granular red mud
Fluoride removal
Adsorption

ABSTRACT

This paper describes the removal of fluoride from water using granular red mud (GRM) according to batch and column adsorption techniques. For the batch technique, the experiments demonstrated that maximum fluoride removal was obtained at a pH of 4.7 and it took 6 h to attain equilibrium and equilibrium time did not depend upon the initial fluoride concentration. Kinetics data were fitted with pseudo-second-order model. The Redlich–Peterson and Freundlich isotherm models better represented the adsorption data in comparison to the Langmuir model. Column experiments were carried out under a constant influent concentration and bed depth, and different flow rates. The capacities of the breakthrough and exhaustion points decreased with increase of the flow rate. Thomas model was applied to the experimental results. The modelled breakthrough curves were obtained, and they were in agreement with the corresponding experimental data. The column adsorption was reversal and the regeneration operation was accomplished by pumping 0.2 M of NaOH through the loaded GRM-column.

1. Introduction

Fluoride in drinking water can be either beneficial or detrimental to health depending on its concentration. Maintaining fluoride concentration of 1 mg/L in the dietary intake can prevent skeletal and dental problems. However, when the fluoride concentration is above this level, it leads to dental and skeletal fluorosis and lesions of the endocrine glands, thyroid and liver. According to the World Health Organization (WHO), the maximum acceptable concentration of fluoride is 1.5 mg/L [1]. It is therefore necessary to remove the excessive fluoride from drinking water if the fluoride concentration is higher than 1.5 mg/L.

Many methods, i.e. adsorption [2,3], ion exchange [4], precipitation [5], Donnan dialysis [6–9], electrodialysis [10,11], reverse osmosis [12], nanofiltration [13] and ultrafiltration [14] have been investigated to remove excessive fluoride from water.

For the treatment of water by adsorption, activated carbon is the most widely used adsorbent. However, it is very expensive and has high operating cost [15]. Therefore, in recent years, considerable attention has been devoted to the study of different types of low-cost materials such as kaolinite, bentonite, charfine, lignites, sirmali seeds [16], calcite [17], amorphous alumina [18], bleaching earth [19], red mud [2], gas concrete material [20], montmorillonite [3], etc., for adsorption of fluoride from water.

Adsorption studies using red mud from alumina refineries as unconventional adsorbent for water and wastewater treatment purposes are motivated by the fact that red mud is a fine-grained mixture of oxides and hydroxides, capable of removing several contaminants, as well as being widely available. An additional advantage for adsorption studies using red mud is that no toxic sludge is produced as a result of pollutant removal and the spent red mud will satisfy the toxicity characteristics leaching procedure (TCLP) criteria for classification as an inert waste. Hence, this classification substantially reduces costs and risks associated with the management of the spent red mud [21,22].

Thus, several studies have reported that red mud or activated red mud can be utilized for adsorbing pollutants, such as dye [23], phenol [24,25], boron [26], phosphate [27], nitrate [28], heavy metals [29,30], arsenic [21,22,31], etc., from water.

Up to now, red mud has been generally used in batch technique because red mud particles are too fine to use in column technique. Therefore, new sorbents, which are red mud-based and suitable for use in column, have been prepared by different workers. For example, Ho et al. [32] used the red mud and sand in columns to remove bacteria and viruses from water. Genç-Fuhrman et al. [33] also developed sea water neutralized red mud (bauxsol) and activated red mud-coated sand and they tested the use of prepared adsorbents for removing arsenic from water with column experi-

* Corresponding author. Tel.: +90 332 223 1914; fax: +90 332 241 0635.
E-mail addresses: ali.alitor@gmail.com, ator@selcuk.edu.tr (A. Tor).

0304-3894/$ – see front matter © 2008 Elsevier B.V. All rights reserved.
doi:10.1016/j.jhazmat.2008.08.011

ments. Zhu et al. [34] prepared the granular red mud (GRM) and evaluated its potential use to remove cadmium ions from water as low-cost adsorbent.

With our knowledge from the literature survey, the removal of fluoride from water by using red mud under continuous flow conditions has not been reported. Therefore, the objective of this study is to: (i) prepare the GRM according to the method reported by Zhu et al. [34], (ii) perform batch studies to examine fluoride adsorption using the GRM, and (iii) perform column studies to investigate the fluoride uptake characteristics of the GRM under different flow rates.

2. Materials and methods

2.1. Chemicals and reagents

All chemicals, including sodium fluoride, sodium chloride, sodium hydroxide, glacial acetic acid, hydrochloric acid, sodium silicate and sodium carbonate were of analytical grade and obtained from Merck Co. (Darmstadt, Germany).

2.2. Preparation of GRM

Utilized raw materials used for granulation, red mud was supplied by Seydisehir Eti Aluminium Plant (Konya) (the grain size of the red mud was mostly >94% less than 10 μm) and fly ash was supplied by the Cement Factory (Konya). Before the granulation procedure, red mud was neutralized as follows. The alkaline red mud was suspended in distilled water with a liquid to solid ratio of 2/1 on a weight basis, stirring it until the equilibrium pH is 8.0–8.5, and drying. Then, GRM was prepared according to the procedure described by Zhu et al. [34]. 15 g of neutralized red mud, 2 g of dried fly ash, 1 g of sodium carbonate, 0.8 g of powdered quicklime and 1.2 g of sodium silicate were mixed until evenly homogenization. Afterwards, some boiling water was added into the mixture until pasting and then granulation was carried out by manual. The obtained granules were dried under environment temperature and moisture for 24 h. Finally, dried granules were roasted and calcined at 400 °C for 2 h and at 900 °C for 0.5 h, respectively. Prepared GRM was sieved and the granules having diameter of 1–1.18 mm were used in the experiments.

2.3. Batch adsorption experiments

The fluoride solutions were prepared by diluting the prepared stock solution (1000 mg/L NaF, prepared in laboratory) to desired concentrations. All experiments were carried out at a constant ionic strength of 0.01 M maintained with NaCl. 0.25 g of GRM and fluoride solution were taken in a 100 mL stoppered conical flask. 5 mL of 0.1 M sodium chloride was added to maintain ionic strength, and pH was adjusted to the desired level with 0.1 M NaOH or 0.1 M HCl solutions. pH of the solution was determined by using ionmeter (Orion EA940, USA). The final volume of the solution was 50 mL. The solution was shaken at constant speed (400 rpm) with shaker at 25 ± 1 °C over a period of time and filtrated with a 0.45 μm cellulose acetate membrane without centrifugation. The amount of fluoride adsorbed was calculated from the following equation:

$$q = \frac{(C_0 - C_e)V}{m} \quad (1)$$

where q is the fluoride adsorbed (mg/g), C_0 is the initial concentration of fluoride (mg/L), C_e is the concentration of fluoride in solution at equilibrium time (mg/L), V is the solution volume (L), and m is the adsorbent dosage (g). The experimental parameters studied are contact time (15–540 min), initial fluoride concentration (5–150 mg/L), and pH (2.5–7.3).

2.4. Column adsorption experiments

GRM is used in continuous flow column to investigate the influence of flow rate on the fluoride removal efficiency and to compare the measured adsorption capacities for the batch and column systems. For this purpose, columns (0.635 cm^2 of cross sectional area and 15 cm of height) are packed with 10 g of GRM and used as fixed bed down-flow reactors (10 cm of bed depth). Influent water is pumped through the packed columns with a peristaltic pump (Labor-Schlauchpumpe PLP 330, Germany). The columns are operated using downward flow at 25 ± 1 °C in the air conditioned laboratory. The distilled water is run through the columns for 5 h prior to starting the experiments in order to wet the columns and to establish equilibrium between the adsorbent and the water.

Flow rates of 2, 3 and 5 mL/min are used to study the effect of the flow rate on fluoride removal. The columns were run using water containing 5 mg/L of fluoride with a pH of 4.7. Flow rates are checked by physically collecting the discharge from column for a given time and measuring the volume collected. After exhaustion of the column, desorption studies are carried out using 0.2 M of NaOH.

The capacity at the breakthrough point (q_B) is defined as the amount of fluoride ions bound by GRM when the concentration of fluoride in the effluent reaches ≈5% of the initial concentration [35].

$$q_B = \int_0^{V_B} \frac{(C_0 - C)\,dV}{m} \quad (2)$$

where q_B is the capacity at the breakthrough point (mg/g), C_0 is the influent fluoride concentration (mg/L), C is the effluent fluoride concentration (mg/L), m is the mass of the sorbent (g), and V_B is the volume of solution passed up to the breakthrough point (L).

The capacity at the exhaustion point (q_E) corresponds to the amount of fluoride ions bound by GRM when the concentration of fluoride in the effluent reaches ≈95% of the initial value [35]:

$$q_E = \int_0^{V_E} \frac{(C_0 - C)\,dV}{m} \quad (3)$$

where q_E is the capacity at the exhaustion point (mg/g), V_E is the volume of solution passed up to the exhaustion point (L), and C_0, C and m are defined as the same as above.

2.5. Column regeneration studies

To retrieve the GRM adsorbents and reuse saturated column, regeneration experiments were conducted by pumping 0.2 M of NaOH as desorption solution through exhausted column. In the present study, the column previously run under "2 mL/min of flow rate" was chosen in desorption experiments on account of representativeness. The regenerated column was then used for the next cycle of column adsorption. All together four cycles of regeneration experiments were conducted until the retained fluoride amount by GRM column are more than the amount recovered by desorption solution. After each cycle of regeneration, the column was washed by distilled water. Taken into consideration the accumulative masses amount by former adsorption cycles, the desorption efficiency E_D is calculated as (for one cycle) [34]

$$E_D\ (\%) = \frac{M_D \cdot 100}{[(q_E m + M_A)]} \quad (4)$$

where q_E and m are defined as the same as above, M_D is the desorption fluoride amount (mg) eluted by desorption solution (0.2 M of

NaOH), and M_A is the fluoride amount (mg) retained in the column that cannot be desorbed.

2.6. Determination of fluoride

The fluoride concentration of the solutions was determined by a fluoride selective electrode (Mettler-Toledo, Switzerland) by use of total ionic strength adjustment buffer (TISAB) solution (58 g of sodium chloride, 57 mL of glacial acetic acid and approximately 150 mL of 6 M NaOH in a volume of 1000 mL) to eliminate the interference effect of other ions. The fluoride samples and the fluoride standard solutions were diluted 1:1 with a TISAB solution [36].

3. Results and discussion

3.1. Characterization of GRM

After preparation of GRM by following the method reported by Zhu et al. [34], the physical and chemical properties of GRM were examined. The chemical composition of the GRM was determined according to the procedure described in Ref. [37] by using ICP-AES (Varian, vista/AX CCD Simultaneous ICP-AES, Australia) and the result was as follows (% by wt.): Al_2O_3: 17.1, Fe_2O_3: 32.4, TiO_2: 4.1, Na_2O: 10.4, CaO: 8.9, SiO_2: 19.2, MgO: 1.1, loss on ignition: 6.8. The surface are of GRM was determined as 10.2 m^2/g according to the published method of Sears [38]. pHzpc (pH of zero point of charge) was also determined as 5.1 by method adopted from Balistrieri and Murray [39]. In addition, Zhu et al. [34] analysed the GRM by XRD and they reported that it was mainly composed of quartz, calcium titanium silicates, sodium aluminosilicates, iron oxides (hematite), and hydroxides and other amorphous minerals.

3.2. Batch adsorption experiments

3.2.1. Effect of pH

The effect of pH on the adsorption of fluoride by using GRM is shown in Table 1. The results showed that adsorption was maximum at a pH of 4.7. The removal was also not favour at a pH below 4.7. This can be attributed to the distribution of F^- and HF which are controlled by pH of the aqueous solution. As can be calculated from Eq. (5) [40], F^- ion is dominant species when pH of the solution is higher than pK_a (3.16) of HF.

$$\varphi_{\text{ions}} = \frac{1}{[1 + 10^{(\text{p}K_a - \text{pH})}]} \quad (5)$$

It is also seen in Table 1 when pH of the solution exceeded 4.7, adsorption also decreased. This may be explained by considering the pHzpc for the GRM. The surface charge of the GRM is assessed by the zero point of charge (pHzpc = 5.1). At pH < pHzpc, the surface charge is positive, at pH = pHzpc, the surface charge is neutral, and at pH > pHzpc, the surface charge is negative. The metal oxides present in GRM form aqua complexes with water and develop a charged surface through amphoteric dissociation. At a pH, above pHzpc, more of the surface sites are negatively charged and F^- will

Table 1
Effect of pH on the adsorption of fluoride by GRM (initial fluoride concentration: 15 mg/L, GRM: 5 g/L, contact time: 8 h, agitation speed: 400 rpm and temperature: 25 ± 1 °C)

pH of the solution	q (mg/g)
2.5	1.211
3.4	1.692
4.7	2.201
5.6	0.872
7.3	0.655

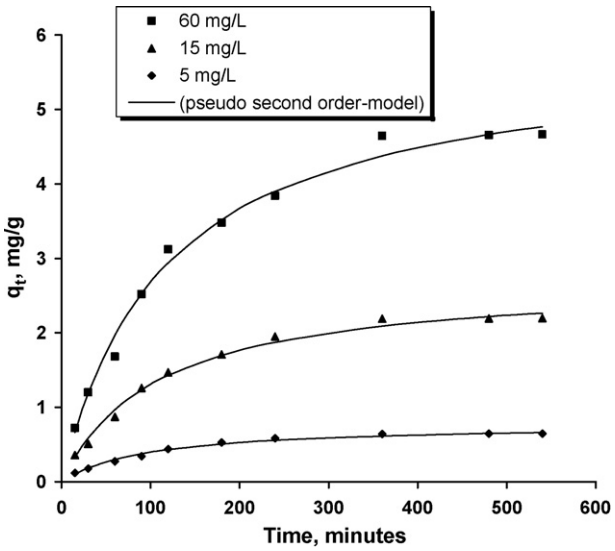

Fig. 1. Effect of contact time on the fluoride removal from water using GRM at 25 ± 1 °C with a pH of 4.7, GRM dosage of 5 g/L and shaking speed of 400 rpm.

be adsorbed to a lesser extent due to the repulsive forces between F^- ions and negative charge of the GRM surface.

At a pH of 4.7, the specific adsorption of fluoride on metal oxides of GRM is due to the electrostatic interaction between positively charged GRM surface and negatively charged fluoride ions and can be modelled as follows [2,3]:

$$\equiv\text{MOH} + \text{H}^+ \Leftrightarrow \equiv\text{MOH}_2{}^+$$

$$\equiv\text{MOH}_2{}^+ + \text{F}^- \Leftrightarrow \equiv\text{MF} + \text{H}_2\text{O},$$

overall reaction can be written as

$$\equiv\text{MOH} + \text{H}^+ + \text{F}^- \Leftrightarrow \equiv\text{MF} + \text{H}_2\text{O}$$

where M represents the metal ion (Si, Fe or Al).

3.2.2. Effect of contact time and adsorption kinetics

The removal of fluoride as a function of contact time is shown in Fig. 1. It was observed that with a fixed amount of GRM, the removal of fluoride increased with time and then attained equilibrium after 360 min. Fig. 1 additionally indicated that the time to reach equilibrium conditions was independent of initial fluoride concentration.

The experimental adsorption data was analysed by application of the pseudo-first-order and pseudo-second-order kinetic models.

The linearized form of pseudo-first-order rate equation is given as [41]

$$\log(q_e - q_t) = \log q_e - \frac{k_1 t}{2.303} \quad (6)$$

where q_e and q_t are the amounts of fluoride adsorbed (mg/g) at equilibrium and at time t (min), respectively, and k_1 (1/min) is the adsorption rate constant of first-order adsorption.

For the studied initial concentrations, the rate constant (k_1) and theoretical equilibrium sorption capacities, q_e (calculated), calculated from the slope and intercept of the linear plots of the pseudo-first-order kinetic model, are given in Table 2. The coefficients of determination (R^2) for the linear plots are between 0.898 and 0.962. In addition, q_e (calculated) and q_e (experimental) values are not in agreement with each other. Therefore, it could be suggested that the adsorption of fluoride by GRM was not a first-order reaction.

Table 2
Values of adsorption rate constant for pseudo-first-order and pseudo-second-order kinetic models

C (mg/L)	q (exp) (mg/g)	Pseudo-first-order kinetic model			Pseudo-second-order kinetic model		
		k_1 (1/min)	q (cal) (mg/g)	R^2	k_2 [g/(mg min)]	q (cal) (mg/g)	R^2
5	0.644	0.012	0.149	0.962	0.013	0.778	0.994
15	2.201	0.010	2.892	0.960	0.003	2.701	0.994
60	4.644	0.002	3.162	0.898	0.002	5.797	0.993

The experimental data was also applied to the pseudo-second-order kinetic model given as

$$\frac{dq_t}{dt} = k_2(q_e - q_t)^2 \quad (7)$$

where k_2 is the rate constant of pseudo-second-order chemisorption (g/(mg min)). For boundary conditions ($t = 0$ to $t = t$ and $q_t = 0$ to $q_t = q_t$), pseudo-second-order kinetic model of Ho and McKay [42,43] is:

$$\frac{t}{q_t} = \frac{1}{(k_2 q_e^2)} + \frac{t}{q_e} \quad (8)$$

For different concentrations of fluoride, the fit of this model was controlled by each linear plot of t/q_t versus t, respectively. The constants calculated from the slope and intercept of the plots are given in Table 2. It can be seen from the results in Table 2 that R^2 values are higher than those obtained from the first-order kinetics. Additionally, theoretical and experimental q_e values are in a good accordance with each other. Therefore, it is possible to suggest that the sorption of fluoride by GRM followed the second-order type reaction kinetics.

After adsorption, the measured final pH values for initial solution pH of 4.7 ranged between 4.9 and 5.1, which indicated that the prepared GRM particles did not cause a release of hydroxyl ions into the solution under acidic conditions.

3.2.3. Adsorption isotherm models

The analysis of the sorption isotherms is important for design purposes. Therefore, experimental data was analysed with well known sorption isotherm models including the Langmuir, Freundlich and Redlich–Peterson isotherms.

Langmuir sorption isotherm models the monolayer coverage of the sorption surfaces and assumes that sorption take places on a structurally homogeneous surface of the adsorbent. This isotherm is given as [44]

$$q_e = \frac{Q_0 b C_e}{(1 + bC_e)} \quad (9)$$

The linear form of the Langmuir isotherm model can be presented as

$$\frac{C_e}{q_e} = \left(\frac{1}{Q_0 b}\right) + \left(\frac{C_e}{q_e}\right) \quad (10)$$

where C_e is the concentration of fluoride (mg/L) at equilibrium, Q_0 is the monolayer capacity of the adsorbent (mg/g) and b is the Langmuir adsorption constant (L/mg). The plot of C_e/q_e versus C_e gives a straight line and the values of Q_0 and b can be calculated from the slope and intercept of the plot, respectively.

Freundlich equation is derived to model the multilayer sorption and for the sorption on heterogeneous surfaces. The Freundlich model is formulated as [45]

$$q_e = kC_e^{1/n} \quad (11)$$

Linearized form of the Freundlich equation is given by the following equation:

$$\log\ q_e = \log\ k + \left(\frac{1}{n}\right)\ \log C_e \quad (12)$$

where C_e is equilibrium concentration (mg/L), k is the sorption capacity (mg/g) and n is an empirical parameter. According to the Eq. (12) the plot of the $\log q_e$ versus $\log C_e$ gives a straight line and k and n values are calculated from the intercept and slope of this straight line, respectively.

The Redlich–Peterson isotherm [46] has a linear dependence on concentration in the numerator and an exponential function in the denominator. It approaches the Freundlich model at high concentrations and is in accord with the low concentration limit of the Langmuir equation. Furthermore, the Redlich–Peterson equation incorporates three parameters into an empirical isotherm, and therefore, can be applied either in homogenous or heterogeneous systems due to its high versatility. The Redlich–Peterson equation is:

$$q_e = \frac{K_R C_e}{(1 + a_R C_e^{\beta})} \quad (13)$$

where K_R is the Redlich–Peterson isotherm constant (L/mg), a_R is also a constant $(L/mg)^{\beta}$ and β is the exponent which lies between 0 and 1. For $\beta = 1$, Eq. (13) reduces to Langmuir equation and for $\beta = 0$, it reduces to Henry's equation. Eq. (13) can be converted to a linear form by taking logarithms:

$$\ln\left[\left(\frac{K_R C_e}{q_e}\right) - 1\right] = \ln a_R + \beta \ln C_e \quad (14)$$

The values of the constants for Redlich–Peterson isotherm were also obtained from the slope and intercept of the plots of linear form of isotherm (Eq. (14)).Fig. 2 shows the Langmuir, Freundlich

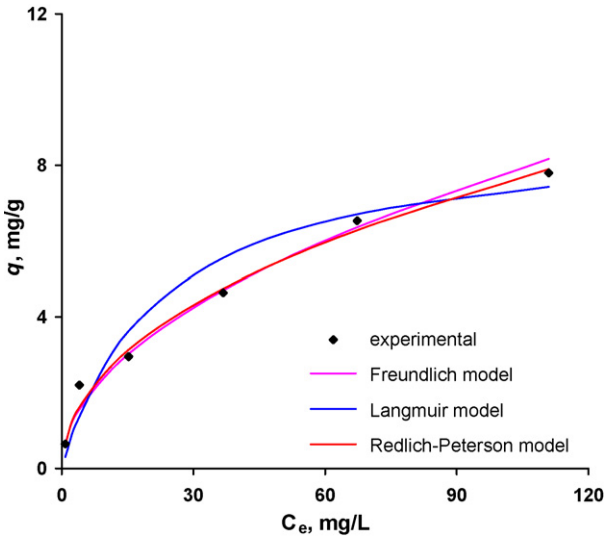

Fig. 2. The Langmuir, Freundlich and Redlich–Peterson isotherms for fluoride adsorption on GRM at 25 ± 1 °C with a pH of 4.7, contact time of 6 h, GRM dosage of 5 g/L and shaking speed of 400 rpm.

Table 3
Langmuir, Freundlich and Redlich–Peterson isotherm parameters for the adsorption of fluoride by GRM

Langmuir isotherm	
Q_0 (mg/g)	8.921
b (L/mg)	0.045
R^2	0.951
Freundlich isotherm	
k (mg/g)	0.851
n	2.082
R^2	0.973
Redlich–Peterson isotherm	
K_R (L/mg)	3.101
a_R (L/mg)$^\beta$	3.089
β	0.580
R^2	0.980

and Redlich–Peterson isotherms and the experimental data. The isotherm constants and R^2 values for each model are given in Table 3.

On the comparison of the R^2 values, it can be concluded that adsorption data can be better described by Redlich–Peterson and Freundlich isotherm models. In fact, for our experimental data, Redlich–Peterson model supported the Freundlich isotherm model. This result can be also inferred from the value of β (0.580), which is lower than unity. This result may be attributed that various active sites or heterogeneous mixture of several minerals on GRM has different affinities to fluoride ion [47]. Cengeloglu et al. [2] reported that the Freundlich isotherm better modelled the adsorption of fluoride onto neutralized red mud, and the neutralized red mud is the raw material of the GRM used in the presented study. The comparison of the Freundlich capacity constants of different adsorbents for fluoride adsorption was given in Table 4.

3.3. Column adsorption experiments

The adsorption columns were operated with different flow rates (2, 3 and 5 mL/min) until no further fluoride removal was observed. The breakthrough curve for a column is determined by plotting the ratio of the C_e/C_0 (C_e and C_0 are the fluoride concentration of effluent and influent, respectively) against the time. A pH deviation of ±0.2 is observed in the influent water for all columns but deviations in effluent water pH up to 0.3 pH units were observed.

During the process, the influent containing fluoride ions passes through the fixed bed of GRM, and a mass transfer zone, where the fresh solution is in contact with unsaturated GRM, forms [50]. This zone also moves through the column and reaches exit at the exhaustion point. The height of the mass transfer zone (h_Z) can be calculated by the following equation [35]:

$$h_z = \frac{H(V_E - V_B)}{[V_E - (1-f)(V_E - V_B)]} \quad (15)$$

Table 4
The comparison of the Freundlich capacity constants of different adsorbents for fluoride adsorption

Adsorbent	k (mg/g)	n	Reference
Neutralized red mud (powdered)	1.14	1.29	[2]
Acid activated red mud (powdered)	5.06	1.97	[2]
Montmorillonite	0.26	1.77	[3]
Spent bleaching earth	0.94	0.46	[19]
Laterite	0.13	1.70	[48]
Manganese-oxide-coated alumina	1.10	3.04	[49]
Alumina	0.42	3.87	[49]
Granular red mud	0.851	2.082	Present study

where H is the bed depth (cm), f is a parameter which measures the symmetry of the breakthrough curve, or the fraction of GRM present in the bed which is still capable of removing fluoride.

The f can be defined as

$$f = \int_0^1 \left(1 - \frac{C}{C_0}\right) d\left[\frac{(V - V_B)}{(V_E - V_B)}\right] = \int_{V_B}^{V_E} \frac{(C_0 - C)\,dV}{C_0(V_E - V_B)} \quad (16)$$

where V is the effluent volume (L) and the others are defined as the same as above.

The empty bed contact time (EBCT) or the residence time is usually defined as the relation between the depth of the GRM bed in the column and the influent velocity:

$$\text{EBCT} = \frac{H}{v} \quad (17)$$

where v is the linear flow rate through the column (cm^3/cm^2 min)

The parameters given by Eqs. (2), (3) and (15)–(17) were calculated from the experimental data and given in Table 5. With increase of flow rates, the empty bed contact time (EBCT) decreased, while the height of the mass transfer zone (h_Z) increased.

The results in Table 5 showed that breakthrough and exhaustion capacities negligibly decreased with increase of flow rates, which is a main factor for practical application of this process.

It is too difficult to describe the dynamic behaviour of compound in a fixed bed under defined operating conditions because the process does not occur at a steady state while the influent still passes through the bed. Various simple mathematical models have been developed to describe and possibly predict the dynamic behaviour of the bed in column performance [51]. One of these models used for the continuous flow conditions is the Thomas model [52], which can be written as

$$\frac{C_e}{C_0} = \frac{1}{(1 + \exp[k_T(q_T m - C_0 V)/\theta])} \quad (18)$$

where C_e is the effluent fluoride concentration (mg/L), C_0 is influent fluoride concentration (mg/L), k_T is the rate constant (L/mg h), θ is the flow rate L/h, q_T is the total sorption capacity (mg/g), V is the throughput volume (L), and m is the mass of adsorbent.

The linearized form of the Thomas model is as follows:

$$\ln\left[\left(\frac{C_0}{C_e}\right) - 1\right] = \left(\frac{k_T q_T m}{\theta}\right) - \left(\frac{k_T C_0 V}{\theta}\right) \quad (19)$$

From experimental data for C_e, C_0, and t at different flow rates, graphical dependences were plotted in Fig. 3. The rate constant (k_T) and the total sorption capacity (q_T) can be determined by from a plot of $\ln[(C_0/C_e) - 1]$ against t at a given flow rate. The model parameters were given in Table 5.

In order to provide an adequate test of the Thomas model equation, the total sorption capacity q_T calculated from the Eq. (19) and q_E calculated from the area above the S-curves up to the saturation point should be close to each other. The agreement of q_T and q_E (Table 5) confirms the applicability of the Thomas model to the examined column system.

Insertion of calculated parameters k_T and q_T into Eq. (18) for time t forms the modelled breakthrough curves which were shown by lines in Fig. 4. The satisfactory fitting of the experimental data and modelled breakthrough curves also supported that mass transport through a column of GRM followed the Thomas model. The rate constant, k_T, increased with increasing the flow rate which indicates that the mass transport resistance decreases. With increase of flow rate, breakthrough time decreased because of faster saturation of the fixed bed (Fig. 5). The mass transport resistance is proportional to axial dispersion and thickness of the liquid film on the particle surface [50]. In the presented study, the flow rates are small enough and their effect on the

Table 5
Parameters calculated from the column experimental data

Flow rate (mL/min)	q_B (mg/g)	q_E (mg/g)	f	h_Z (cm)	EBCT (min)	From Thomas model	
						k_T (L/mg h)	q_T (mg/g)
2	1.274	2.051	0.394	4.671	6.369	0.067	1.801
3	1.002	1.909	0.491	6.231	4.246	0.079	1.502
5	0.773	1.490	0.501	6.336	2.548	0.192	1.216

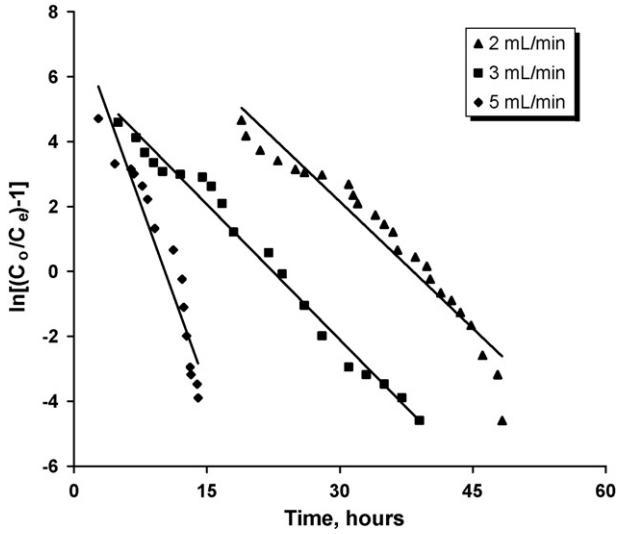

Fig. 3. Testing of experimental results by the Thomas equation.

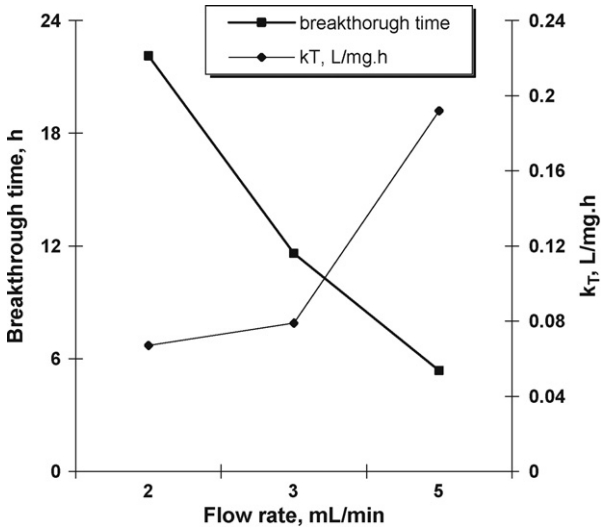

Fig. 5. Dependence of rate constant of the Thomas model and breakthrough time on the flow rate.

increase of axial dispersion is negligible, which is confirmed by the increase of the rate constant. Therefore, it can be assumed that the increase of the flow rate increases the driving force of mass transfer in the liquid film. The results presented show that the Thomas equation can be used to predict the breakthrough curves for fluoride removal by a fixed bed of GRM with different flow rates.

Additionally, the results show that the sorption capacities of the columns are higher than their respective batch capacities (q_e = 0.644 mg/g for 5 g/L GRM dosage) for the same initial fluoride concentration (5 mg/L). Similar results were observed by Genç-Fuhrman et al. [33] and Gupta et al. [53]. The reason for the observed discrepancies between the batch and column systems may be that GRM have pores that favour enhanced solidstate diffusion relative to the batch tests [54].

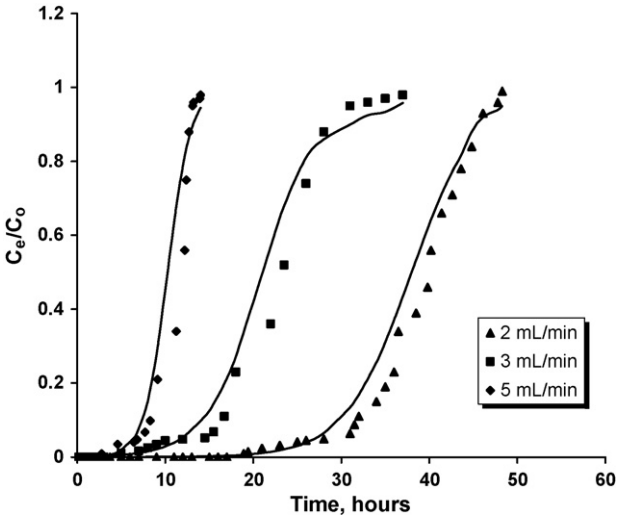

Fig. 4. Breakthrough curves expressed as C_e/C_0 versus time. Fitting of experimental data (points) to curves obtained from the Thomas model (lines).

3.3.1. Column regeneration

When the sorbent was saturated with fluoride, a simple test was carried out to see whether the columns could be chemically regenerated. The exhausted fixed bed column previously run under "2 mL/min" was regenerated by passing 0.2 M of NaOH with a flow rate of 1 mL/min downwards through the bed. The desorption masses was calculated in the way identical to calculation of the column adsorption amounts.

The calculated column desorption parameters were listed in Table 6. Each cycle of the consecutive desorption tests was conducted until no fluoride could be desorbed which was needed 100 mL of desorption solution. It was found that the regenerated GRM column could be utilized for four cycles until completely exhausted. Due to the loss of adsorption capability of GRM column, the regeneration efficiency decreased with the consecutive adsorption cycle accordingly as less fluoride can be desorbed from the GRM column. The concentrated fluoride in the desorption solution can be precipitated using lime. This will probably lead to an

Table 6
Column regeneration parameters for GRM column (adsorption operation condition—influent fluoride concentration: 5 mg/L, flow rate: 2 mL/min, desorption condition—desorption solution 0.2 M of NaOH, solution flow rate 1 mL/min)

Regeneration cycle	q_E (mg/g)	E_D (%)
1	2.051	87
2	1.730	76
3	1.311	58
4	0.824	46

economical process for treatment of concentrated fluoride solution [55].

4. Conclusion

In this study, GRM is prepared and its fluoride sorption capacity is evaluated according to the batch and column adsorption experiments. The main conclusions from this study can be listed as follows:

(i) The high capability of removing fluoride at low concentrations, satisfactory adsorption capacity in batch and column adsorption and fine reversibility to be regenerated rapidly for four cycles indicate that GRM can be used in fluoride adsorption as an upgraded product for powdered red mud adsorbent.
(ii) Batch experiments indicate that the time to attain equilibrium was 6 h and adsorption was followed the pseudo-second-order kinetic model.
(iii) Maximum adsorption or removal of fluoride was achieved at a pH of 4.7.
(iv) The adsorption of fluoride by GRM in batch systems can be described by the Freundlich isotherm, and the adsorption capacity (k) was 0.851 mg/g.
(v) Higher fluoride sorption capacity is obtained using column experiments than using batch experiments.
(vi) The breakthrough capacities (q_B) and exhaustion capacities (q_E) decreased with increase of flow rate.
(vii) The height of the mass transfer zone (h_Z) increased and the empty bed contact time (EBCT) decreased with increase of flow rates.
(viii) Thomas model can be used for predicting of breakthrough curves for fluoride removal by a fixed bed of GRM for different flow rates.
(ix) The rate constant (k_T) increased and the breakthrough time decreased with the increase of the flow rate. This is explained by increased mass transport through the liquid film on the adsorbent surface and faster saturation of the bed.
(x) The fluoride-loaded GRM can be regenerated four cycles after each cycle of adsorption.

Acknowledgement

The authors are grateful for kindly financial support provided by Selcuk University Research Foundation (SUAF).

References

[1] WHO (World Health Organization), Guidelines for Drinking Water Quality, World Health Organization, Geneva, 1993.
[2] Y. Cengeloglu, E. Kir, M. Ersoz, Removal of fluoride from aqueous solution by using red mud, Sep. Purif. Technol. (2002) 81–86.
[3] A. Tor, Removal of fluoride from an aqueous solution by using montmorillonite, Desalination 201 (2006) 267–276.
[4] S. Meenakshi, N. Viswanathan, Identification of selective ion-exchange resin for fluoride sorption, J. Colloid Interface Sci. 308 (2007) 438–450.
[5] M.G. Sujana, R.S. Thakur, S.N. Das, S.B. Rao, Defluorination of waste waters, Asian J. Chem. 4 (1997) 561–570.
[6] F. Durmaz, H. Kara, Y. Cengeloglu, M. Ersoz, Fluoride removal by Donnan dialysis with anion exchange membranes, Desalination 177 (2005) 51–57.
[7] A. Tor, Removal of fluoride from water using anion-exchange membrane under Donnan dialysis condition, J. Hazard. Mater. 141 (2006) 814–818.
[8] E. Kir, E. Alkan, Fluoride removal by Donnan dialysis with plasma-modified and unmodified anion-exchange membranes, Desalination 197 (2006) 217–224.
[9] M. Hichour, F. Persin, J. Sandeaux, C. Gavach, Fluoride removal from waters by Donnan dialysis, Sep. Purif. Technol. 18 (2000) 1–11.
[10] M. Zeni, R. Riveros, K. Melo, R. Primieri, S. Lorenzini, Study on fluoride reduction in artesian well—water from electrodialysis process, Desalination 185 (2005) 241–244.
[11] N. Kabay, O. Arar, S. Samatya, U. Yuksel, M. Yuksel, Separation of fluoride from aqueous solution by electrodialysis: effect of process parameters and other ionic species, J. Hazard. Mater. 153 (2008) 107–113.
[12] S. Sourirajan, T. Matsurra, Studies on reverse osmosis for water pollution control, Water Res. 6 (1972) 1073–1086.
[13] R. Simons, Trace element removal from ash dam waters by nanofiltration and diffusion dialysis, Desalination 89 (1993) 325–341.
[14] L. Guo, B.J. Hunt, P.H. Santsci, Ultrafiltration behavior of major ions (Na, Ca, Mg, F, Cl, and SO_4) in natural waters, Water Res. 35 (6) (2001) 1500–1508.
[15] R. Gong, Y. Ding, M. Li, C. Yang, H. Liu, Y. Sun, Utilization of powdered peanut hull as biosorbent for removal of anionic dyes from aqueous solution, Dyes Pigments 64 (2005) 187–192.
[16] M. Srimurali, A. Pragathi, J. Karthikeyan, A study on removal of fluorides from drinking water by adsorption onto low-cost materials, Environ. Pollut. 99 (1998) 285–289.
[17] M. Yang, T. Hashimoto, N. Hoshi, H. Myoga, Fluoride removal in a fixed bed packed with granular calcite, Water Res. 33 (1999) 3395–3402.
[18] Y.H. Li, S. Wang, A. Cao, D. Zhao, X. Zhang, C. Xu, Z. Luan, D. Ruan, J. Liang, D. Wu, B. Wei, Adsorption of fluoride from water by amorphous alumina supported on carbon nanotubes, Chem. Phys. Lett. 350 (2001) 412–416.
[19] M. Mahramanlioglu, I. Kizilcikli, I.O. Bicer, Adsorption of fluoride from aqueous solution by acid treated spent bleaching earth, J. Flourine Chem. 115 (2002) 41–47.
[20] E. Oguz, Adsorption of fluoride on gas concrete materials, J. Hazard. Mater. 117 (2005) 227–233.
[21] H. Genc, J.C. Tjell, D. McConchie, R.D. Schuiling, Adsorption of arsenate from water using neutralized red mud, J. Colloid Interface Sci. 264 (2003) 327–334.
[22] H. Genç-Fuhrman, J.C. Tjell, D. McConchie, Increasing the arsenate adsorption capacity of neutralized red mud (Bauxsol), J. Colloid Interface Sci. 271 (2004) 313–320.
[23] A. Tor, Y. Cengeloglu, Adsorptive removal congo red from water onto acid activated red mud, J. Hazard. Mater. 138 (2006) 409–415.
[24] A. Tor, Y. Cengeloglu, M.E. Aydin, M. Ersoz, Removal of phenol from aqueous phase by using neutralized red mud, J. Colloid Interface Sci. 300 (2006) 498–503.
[25] A. Tor, Y. Cengeloglu, M. Ersoz, Increasing the phenol adsorption capacity of neutralized red mud by application of acid activation procedure, Desalination, in press.
[26] Y. Cengeloglu, A. Tor, G. Arslan, M. Ersoz, S. Gezgin, Removal of boron from aqueous solution by using neutralized red mud, J. Hazard. Mater. 142 (2007) 412–417.
[27] J. Pradhan, J. Das, S. Das, J. Thakur, Adsorption of phosphate from aqueous solution using activated red mud, J. Colloid Interface Sci. 204 (1998) 169–172.
[28] Y. Cengeloglu, A. Tor, M. Ersoz, G. Arslan, Removal of nitrate from aqueous phase by using red mud, Sep. Purif. Technol. 51 (2006) 374–378.
[29] R. Apak, K. Guclu, M.H. Turgut, Modeling of copper (II), cadmium (II), and lead (II) adsorption on red mud, J. Colloid Interface Sci. 203 (1998) 122–130.
[30] R. Apak, E. Tütem, M. Hügül, J. Hizal, Heavy metal cation retention by unconventional sorbents (red muds and fly ashes), Water Res. 32 (1997) 430–440.
[31] H.S. Altundogan, S. Altundogan, F. Tumen, M. Bildik, Arsenic adsorption from aqueous solutions by activated red mud, Waste Manage. 22 (2002) 357–363.
[32] G.E. Ho, R.A. Gibbs, K. Mathew, Bacteria and virus removal from secondary effluent in sand and red mud columns, Water Sci. Technol. 23 (1991) 261–270.
[33] H. Genç-Fuhrman, H. Bregnhøj, D. McConchie, Arsenate removal from water using sand–red mud columns, Water Res. 39 (2005) 2944–2954.
[34] C. Zhu, Z. Luan, Y. Wang, X. Shan, Removal of cadmium from aqueous solutions by adsorption on granular red mud (GRM), Sep. Purif. Technol. 57 (2007) 161–169.
[35] L.D. Benefield, J.F. Judkins, B.L. Weand, Process Chemistry for Water and Wastewater Treatment, Prentice-Hall, Inc., New Jersey, 1982.
[36] J.H. Kennedy, Analytical Chemistry Principles, 2nd ed., W.B. Saunders, New York, 1990.
[37] E. Kir, Recovery of metals from red mud and investigation on the evaluation of these recovered metals, PhD Thesis, Selcuk University, 2002 (in Turkish).
[38] G. Sears, Determination of specific surface area of colloidal silica by titration with sodium hydroxide, Anal. Chem. 28 (1956) 1981–1983.
[39] L.S. Balistrieri, J.W. Murray, The surface chemistry of goethite (alpha FeOOH) in major ion seawater, J. Am. Sci. 281 (1981) 788–806.
[40] N. Calace, E. Nardi, B.M. Petronio, M. Pietroletti, Adsorption of phenols by papermill sludges, Environ. Pollut. 118 (2002) 315–319.
[41] S. Lagergren, K. Svenska, About the theory of so called adsorption of soluble substances, K. Sven. Vetenskapsad. Handl. 24 (4) (1898) 1–39.
[42] Y.S. Ho, G. McKay, Pseudo-second order model for sorption processes, Process Biochem. 34 (1999) 451–465.
[43] G. McKay, The adsorption of basic dye onto silica from aqueous solution—solid diffusion model, Chem. Eng. Sci. 39 (1984) 129–138.
[44] I. Langmuir, The constitution and fundamental properties of solids and liquids, J. Am. Chem. Soc. 38 (1916) 2221–2295.
[45] H.M.F. Freundlich, Über die adsorption in losungen, Z. Phys. Chem. 57A (1906) 385–470.
[46] O. Redlich, D.L. Peterson, A useful adsorption isotherm, J. Phys. Chem. 63 (1959) 1024.
[47] H. Genç-Fuhrman, J.C. Tjell, D. McConchie, Adsorption of arsenic from water using activated neutralized red mud, Environ. Sci. Technol. 38 (2004) 2428–2434.

[48] M. Sarkar, A. Banerjee, P.P. Pramanick, A.R. Sarkar, Use of laterite for the removal of fluoride from contaminated drinking water, J. Colloid Interface Sci. 302 (2006) 432–441.
[49] S.M. Maliyekkal, A.K. Sharma, L. Philip, Manganese-oxide-coated alumina: a promising sorbent for defluoridation of water, Water Res. 40 (2006) 3497–3506.
[50] N. Vukojevic Medvidovic, J. Peric, M. Trgo, M.N. Muzek, Removal of lead ions by fixed bed of clinoptilolite—the effect of flow rate, Sep. Purif. Technol. 49 (2006) 298–304.
[51] Z. Aksu, F. Gonen, Biosorption of phenol by immobilized activated sludge in a continuous packed bed: prediction of breakthrough curves, Process Biochem. 39 (2004) 599–613.
[52] H.C. Thomas, Heterogeneous ion exchange in a flowing system, J. Am. Chem. Soc. 66 (1944) 1664–1666.
[53] V. Gupta, M. Gupta, S. Sharma, Process development for the removal of lead and chromium from aqueous solutions using red mud, an aluminium industry waste, Water Res. 35 (2001) 1125–1134.
[54] E. Lopez, B. Soto, M. Arias, A. Nunez, D. Rubinos, M.T. Barral, Adsorbent properties of red mud and its use for wastewater treatment, Water Res. 32 (1998) 1314–1322.
[55] A.M. Raichur, M.J. Basu, Adsorption of fluoride onto mixed rare earth oxides, Sep. Purif. Technol. 24 (2001) 121–127.